International Journal of Geosciences, 2016, 7, 120-134
Published Online February 2016 in SciRes. http://www.scirp.org/journal/ijg
http://dx.doi.org/10.4236/ijg.2016.72010

Scientific Research Publishing

The Role of the Southern Hemisphere Polar Cell on Antarctic Sea Ice Variability

Praveen Rao Teleti*, Alvarinho J. Luis

Earth System Science Organization, National Centre for Antarctic and Ocean Research, Ministry of Earth Sciences, Govt. of India, Headland Sada, Goa, India
Email: *praveenrao.teleti@gmail.com

Received 25 December 2015; accepted 21 February 2016; published 24 February 2016

Abstract

The study explores modes of variability in the Southern Polar Cell and their relationship with known global climate modes and Antarctic sea ice. It is found that Polar Cell is barotropic in nature and 500 hPa geo-potential height (Z_{500}) field can satisfactorily represent variability in the Polar Cell. First, three leading Empirical Orthogonal Function (EOF) modes of Z_{500} account for nearly 80% of observed variability in the Polar Cell. Dominant mode ($PC1_{500}$) comprises of high pressure divergence zone over Antarctica. Second leading mode ($PC2_{500}$) is low pressure zone covering Amundsen-Bellingshausen Sea (ABS) similar to ABS low feature. A new climate mode called Polar Coastal Index (PCI) is defined, which describes more than 15% and close to 30% variability of circumpolar trough and ABS low, respectively. Out of four modes defined in this study, only PCI and $PC2_{500}$ show linear trends and clear seasonality. Interestingly, both modes are affected by modulation of ABS low due to tropical ENSO forcing. SAM signature is present in Polar Cell as $PC1_{500}$ shares large variance with it. The largest impact on sea ice comes from $PC2_{500}$ followed by $PC1_{500}$ in the Antarctic Dipole regions. However, this study suggests contemporary sea ice trends cannot be sustained, and can reverse given that trends in PCI and $PC2_{500}$ favour a reversal. These results indicate that ENSO-driven Polar Cell variability plays a crucial role influencing Antarctic sea ice as it interacts with other climate modes and leads the combined impact at the interannual time scale.

Keywords

Antarctica, Sea Ice, Polar Cell, PCI, ENSO, Teleconnection

*Corresponding author.

How to cite this paper: Teleti, P.R. and Luis, A.J. (2016) The Role of the Southern Hemisphere Polar Cell on Antarctic Sea Ice Variability. *International Journal of Geosciences*, **7**, 120-134. http://dx.doi.org/10.4236/ijg.2016.72010

1. Introduction

The atmospheric circulation in the Southern Hemisphere (SH) has a large impact on SH climate and sea ice cover through complex air-ocean-sea ice interaction. Previous studies have identified the hemispheric-scale atmospheric variability in SH comprising of a dominant mode characterized by zonally symmetric see-saw pattern between the mid- and high-latitudes. This mode appears as the leading mode of many atmospheric variables, e.g., mean sea level pressure (MSLP), geopotential heights, zonal winds [1]-[6], which has been referred to as Antarctic Oscillation (AAO) or Southern Annular Mode (SAM) and dominates the region poleward of 20˚S [1] [2] [7] [8]. Second and third modes are identified as the El Niño-Southern Oscillation (ENSO)-driven Pacific-South America (PSA) teleconnection patterns [6]. These modes are part of a stationary wave train generated by tropical convection that travels towards Polar regions.

Aforementioned studies have focused on the role of global climate indices and circulation cells on Antarctic climate and sea ice. However understanding of Southern Polar Cell's impact on sea ice system has been fragmentary. Though the impact of Ferrel Cell variability is well documented, as Marshall [9] provided station-based SAM time-series as a see-saw pattern in Ferrel Cell which circulated in the region bounded by mid-latitudes (~30˚S) in the north and Antarctic coast (~65˚S) in the south, there is a significant knowledge gap in the understanding on how the local circulation cell—the Polar Cell—modulates seasonal and interannual Antarctic sea-ice variability. In this study, we focus on the impact of the local atmospheric circulation pattern due to its immediate interaction with and in vicinity of sea ice. Moreover, several studies have suggested that local climate and circulation might have a larger role in modulating the sea ice variability [10]-[17].

This study attempts to identify the modes of variability in the Polar Cell (region polewards of 65˚S). We perform empirical orthogonal function (EOF) analysis on geopotential height anomalies south of 65˚S, in order to highlight the dominant circulation patterns over Antarctic continent and establish its relationship with the observed sea ice changes (e.g., [13] [18]). The Polar Cell is characterized by intense surface divergence at the South Pole (SP) and a convective zone at the Antarctic coast. Hence, a strong pressure gradient forms between high-altitude Antarctic plateau and Antarctic coastal region that drives air circulation in the Polar Cell. However, previous studies have investigated air mass movement in and out of Polar Cell, which is known as the semiannual oscillation (SAO; [19] [20]) that is characterised by bi-annual transfer of air masses between the Antarctic and mid-latitudes [21]. It is manifested by the changes in the position and strength of the Antarctic circumpolar trough (CPT), lying between 60˚ - 65˚S, which has major impact on Antarctic climate and sea ice.

In SAO studies, the choice of latitude bands (50˚ - 65˚S) selected for its computation does not capture the full variability of forces which drives intra-cell circulation in the Polar Cell. Hence, we propose a new polar-coastal pressure gradient index called the Polar Coastal Index (PCI) which is defined as normalized MSLP difference between 65˚S and 90˚S. It is similar to the SAO, but the important difference between PCI and SAO is that the former accounts for strong pressure gradient between SP and Antarctic coast which drives most of the Polar Cell circulation and the CPT, whereas the SAO measures air masses movement between 50˚S and 65˚S (peripheral ocean).

We employ reanalysis products (description of all datasets in Section 2) and use EOF techniques to study the atmospheric variability. As would be shown in results (Section 3), the PCI could explain more than 15% variability observed in the CPT and about 30% of the Amundsen-Bellingshausen Sea Low (ABSL) variability [22]. Essentially PCI is a measure of the CPT variability and hence coastal winds. Studies have shown that these surface wind fields [12] [13] and near-shore winds [23] play a major role in the convective processes and exchange of heat and momentum with ocean. We attempt to investigate modes of variability in the Polar Cell and its relationship with the above mentioned global climate mode indices. We will characterise dominant modes of Polar Cell in relationship with Antarctic sea ice concentration. We employ lead-lag correlation analysis for each climate indices with sea ice, in order to explore causation impact on each other. As dominant modes are extracted from geopotential height anomalies and PCI is generated from MSLP field this procedure will provide us with more information on variability of the Polar Cell across atmospheric levels. We discuss the findings and offer conclusions in section 4.

2. Data and Methods

The sea ice concentration (SIC) with a spatial resolution of 25 × 25 km was obtained from the National Snow and Ice Data Center. The monthly SIC spanning 1979-2013 were computed by using the NASA Team algorithm

[24] which were obtained from SMMR, SSMI, and SSMIS observations. The data used to examine circulation features are monthly mean geopotential heights derived from National Centers for Environmental Prediction-Department of Energy (NCEP-DOE) Reanalysis 2 (NCEP2) dataset [25]. It is an updated and improved version of the widely used NCEP-NCAR data, assimilated with global satellite soundings network data. The horizontal resolution is 2.5˚ × 2.5˚ and the study period spans 1979 to 2013.

To capture the essential features of Polar Cell, we apply EOF or principal component (PC) analysis to separate observed variability into orthogonal modes, each consists of a spatial pattern and a time series. Before carrying out the EOF analysis the data was processed as follows. First, annual cycle was removed from the datasets by subtracting climatological monthly means from individual months. Second, to ensure equal area weighting for the covariance matrix, the gridded data was weighted by the square root of the cosine of latitude to obtain the EOF loading patterns. The modes are arranged in the descending order of variance explained by them, *i.e.*, the first PC explains more variance than second and so on. The primary modes of variability in the Polar Cell is defined as the first three leading modes of monthly height anomalies at 500 hPa (Z_{500}), 800 hPa (Z_{800}), MSLP in region poleward of 65˚S. Monthly time series of PCs are constructed by projecting the monthly mean anomalies onto the modes. The normalized PC time series have the same units as the anomaly field hence dimensionless.

PCI Computation

The variability in the Polar Cell can be extracted by considering two extremes of its circulation, thus the PCI pattern is most profound feature in MSLP field, e.g. average MSLP values over continental Antarctica and coastal region differ by 37.5 hPa over the study period. Monthly PCI was computed from NCEP2 by subtracting normalised MSLP at 65˚S (Antarctic coast) from 90˚S (SP) (**Figure 1(d)**). The ENSO/Southern Oscillation Index (SOI) was obtained from NOAA (http://www.cpc.ncep.noaa.gov/data/indices/soi) and the SAM time series was obtained from British Antarctic Survey (http://www.nerc-bas.ac.uk/icd/gjma/sam.html).

The time series of these EOF modes and PCI were standardized and lines of least squares fit were fitted to quantify trends. The trend over 34 years was determined as the difference between the values at the two end-points of the least-squares-fit line divided by the number of years. The long-term trend was removed at each SIC grid point and from each of the indices before computing the correlation coefficients which were judged at 99% significance level by using the standard Student *t*-test. To focus on interannual and longer timescales, we filtered the monthly time series of climate indices and sea ice anomalies with a low pass filter, an infinite impulse response (IIR) filter with cut-off threshold at 13-month. All time-series are filtered unless otherwise stated.

3. Results

3.1. Modes of Variability in SH Polar Cell

The spatial pattern of first three leading modes of MSLP, Z_{800} and Z_{500} are very similar (**Figure S1**), and also their time series show high correlation (**Table 1**). Total variance explained by first three modes of each variable MSLP, Z_{800} and Z_{500} are 70%, 78% and 79%, respectively. It is apparent that Polar Cell is barotropic, hence we will use modes of Z500 field to define Polar Cell variability as it explains more variability than any other

Table 1. Cross-correlation between PC's of Z_{500}, MSLP and Z_{800}, all are significant at 99% level (shared variance in percentages).

PC's	Cross-correlation		
	$PC1_{500}$	$PC2_{500}$	$PC3_{500}$
$PC1_{MSLP}$	0.72 (51.84%)	--	--
$PC2_{MSLP}$	--	−0.81 (65.61%)	--
$PC3_{MSLP}$	--	--	−0.78 (61%)
$PC1_{800}$	0.91 (83.28%)	--	--
$PC2_{800}$	--	0.96 (91.96%)	--
$PC3_{800}$	--	--	0.96 (92.94%)

field. Spatial pattern of first three PCs of Z_{500} covers important features contained in Polar Cell (**Figure 1**), such as a high-pressure over Antarctic continent and a low pressure zone over Amundsen Sea and Antarctic Peninsula (AP).

Leading PC ($PC1_{500}$) pattern which explains more than 50% of the variability shows anomalous negative values all over Antarctica with three main lobes near coast of Amundsen Sea and high-altitude East Antarctic plateau region. High pressure zone is expected in this region due to permanent cold temperatures, high-altitude and Polar divergence. This quasi-permanent anomaly affects circulation over entire continental Antarctica and divergence zone results in lowest recorded precipitation in these regions (**Figure S2(a)**).

The second dominant mode ($PC2_{500}$) explains ~14% of variability and shows a pattern of low pressure zone, as positive anomalous heights in the Amundsen and Bellingshaushen Seas (ABS) (similar to ABS Low) and negative anomalies in the East Antarctica. Reference [26] pointed out that the low in ABS exists because of the asymmetrical topography of AP and Antarctic continent which actively influence the air circulation in the region. It's also been suggested that ABSL strength is influenced by large-scale patterns of climate variability, namely SAM [22] and ENSO [27] [28]. However, the interaction between these climate modes and topographic conditions, which dictates strength and position of the ABSL, are not yet clear.

The third dominant mode ($PC3_{500}$), explains ~10% variability, with anomalous positive values moving to AP region. Reference [29] investigated large number of cyclogenesis events which take place within this low pressure zone (around AP) between the latitudes of 60˚ and 70˚S. They pointed out that the main mechanism behind

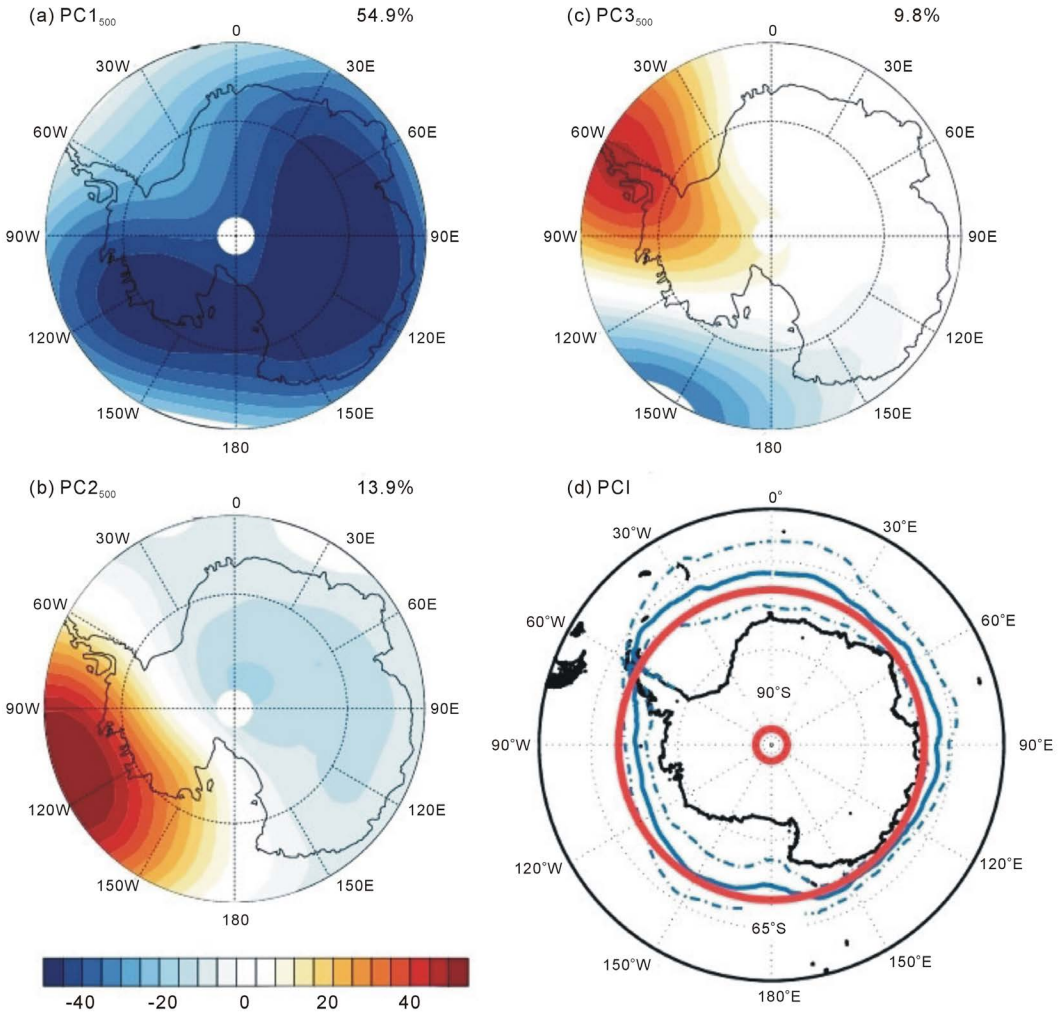

Figure 1. Spatial pattern of first three leading modes of Z500 (a) $PC1_{500}$ (b) $PC2_{500}$ (c) $PC3_{500}$ and (d) latitude bands used to calculate PCI (red lines), mean sea ice edge (solid blue) and $\pm 1\sigma$ (dashed blue).

meso-cyclones developments were the lows, which are formed inside pre-existing low pressure zone in the AP region, from which synoptic-scale cyclonic weather systems emerges leading to large cyclone density. This cyclonic activity due to deeper lows has significant impact on local climate and sea-ice conditions around AP.

Lastly, the PCI, which describes essentially zonal mode in the Antarctic coastal region, is characterized by the bi-annual heightened meridional pressure gradient similar to SAO [30]-[32] which is due to difference in heating of the Antarctic continent and the coastal region. This influence is also visible in the spatial pattern of PCI regression on MSLP field, in which the PCI accounts for more than 15% variability in much of the Antarctic coastal region (e.g., CPT), except for AP. Since, more than 30% variability can be accounted in Amundsen Sea and Ross Sea regions, we suggest that PCI can be used as a reliable proxy to measure variability in the CPT and especially for ABSL phenomena (**Figure 2(a)**). The low percentage of the variance explained by PCI over the Antarctic continent implies that $PC1_{500}$ or combination of higher order modes is likely dominant there. Therefore, PCI can vary across the latitudes around the region that it affects, both in terms of strength and extent. Seasonal variations in these modes and PCI are discussed below.

3.2. Seasonality of Modes

From January till onset of winter season (Jun-Jul-Aug), $PC1_{500}$ weakens (**Figure 2(b)**), as Antarctic continent is heated up due to large incoming solar radiation, pressures over continent are lower than average; it only peaks in

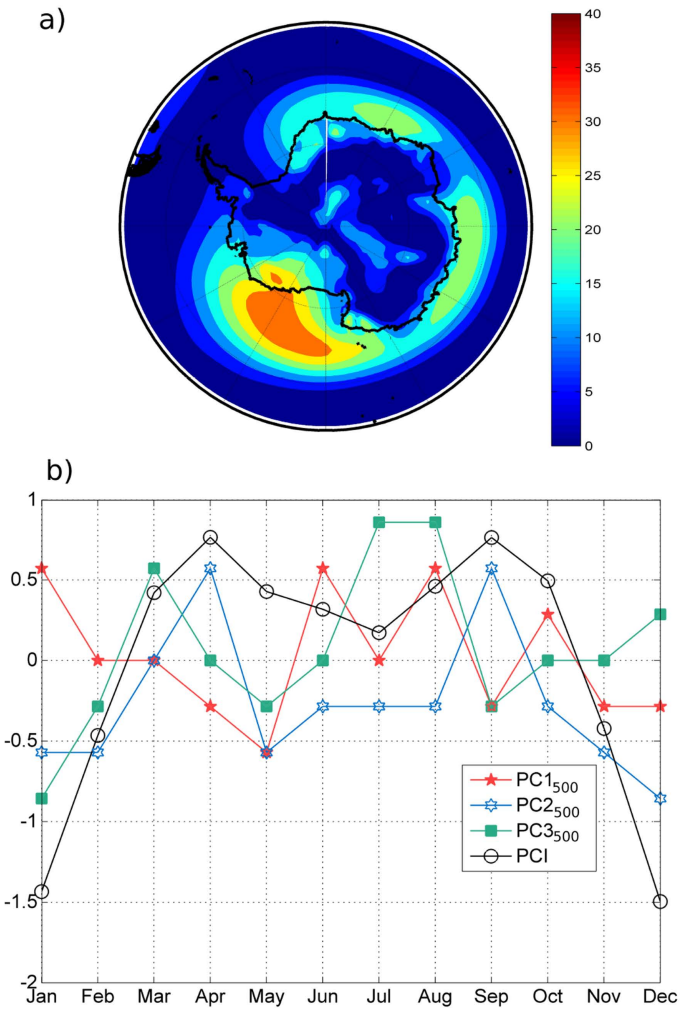

Figure 2. (a) Spatial distribution of MSLP field variance explained by PCI in percentages (%), and (b) Seasonal variations of first three leading modes and PCI.

winter season when extremely low temperatures return. $PC2_{500}$ follows half-yearly cycle, which is mainly due to fall and rise in the strength of ABSL. As ABSL strengthens in autumn (Mar-Apr-May) and spring (Sep-Oct-Nov) $PC2_{500}$ follows it closely. However, $PC3_{500}$ shows an asymmetric cycle—it peaks in March and in winter months (Jul-Aug), and dips in May and September between these two peaks. It can be explained as follows. After period of large solar radiance at the end of summer season, AP region is heated hence $PC3_{500}$ index is positive. Again when winter sets in, the CPT contracts and a low pressure zone is created which brings AP region under the influence of westerlies, which is mild maritime air from the north or north-west as found by [29].

The PCI is overwhelmingly dominated by half-year cycle like SAO depicting two peaks and two troughs. The PCI represents a bi-annual spread and tightening of CPT, which exhibits a minimum pressure and extends furthest south in the autumn and spring seasons (**Figure 2(b)**). This pattern occurs due to difference in the heat capacity of the Antarctic and the Southern Ocean; the shift in air-masses described by PCI strives to equalise the intra-cell imbalance. The PCI is associated with the sub-polar convergence zone which exerts influence over the stages of sea ice advance and retreat cycles [17] [33]. The changes in PCI will have a direct impact on the chronological phases of sea ice formation and melting.

3.3. Trends in Climate Mode Indices

Significant trends exist only in two climate mode indices (PCI and $PC2_{500}$). Apparently, the trend in PCI (0.21 per decade, $p < 0.01$) is the largest, followed by $PC2_{500}$ (−0.16 per decade, $p < 0.01$) (**Figure 3(a)** and **Figure 3(b)**). The positive trend in PCI could mean a deeper CPT and/or stronger high pressure at SP. Our results concurs with the finding of reference [22] who pointed out that MSLP has decreased all around the CPT. Moreover, the cooling of East Antarctica due to loss of stratospheric ozone [34] has also been attributed to changes in SAM. Reference [35] pointed out that cooling could be due to alterations to the circumpolar vortex. All these studies point to favourable conditions in which PCI will have positive trend.

A strong trend in $PC2_{500}$ also indicates an increasingly lower pressure over ABS (e.g., ABSL) and higher pressure over East Antarctic elevated plateau. Proposed mechanisms for Antarctic cooling has been mentioned above and also Reference [22] pointed out that over 1979-2008 period, the ABSL has deepened in spring and autumn. We conclude that simultaneous deepening of ABSL and cooling over Antarctic plateau has resulted in the observed $PC2_{500}$ trend. Overall, simultaneous warming in the AP and cooling over Antarctic plateau is related to broader changes in atmospheric circulation (e.g., SAM) and changes in sea ice [36] [37].

Both PCI and $PC2_{500}$ trends could result from ever more coherent ABSL response to ENSO cold events [38] [27]. This is expected as both modes draw their existence from CPT in case of former and ABSL for later. It can be argued that deepening of CPT (or ABSL) will provide reinforcement for these two modes ($PC2_{500}$ and PCI).

3.4. Is Variability in Polar Cell Related to Other Climatic Modes?

To investigate inter-relationship between known climate modes of SH and variability in Polar Cell, we use correlation analysis. **Figure 3(a)** shows that the correlation between SAM and $PC1_{500}$ is quite strong ($R = 0.69$, $p < 0.01$), indeed $PC1_{500}$ is a manifestation of SAM in the Polar Cell. This result extends observation made by previous studies that, SAM is a dominant mode of variability in the SH including Polar Cell. It is interesting to note that $PC1_{500}$ and PCI ($R = 0.32$, $p < 0.01$) are not strongly correlated suggesting that both represent independent variability in the Polar Cell, which can be attributed to the difference in spatial structure of $PC1_{500}$ and PCI (**Figure 1(a)**, **Figure 1(d)**). Also, SAM is highly correlated with PCI ($R = 0.62$, $p < 0.01$). The PCI and SAM describe similar zonal modes of pressure gradients in high latitudes. PCI is a measure of the pressure gradient between 90˚S and 65˚S, while SAM represents pressure difference between 40˚S and 65˚S; so both indices share one region in common. Both indices owe their existence to movement of air masses, back and forth from mid-latitude to coastal Antarctica in the case of SAM, and from coastal Antarctica to elevated Antarctic region in the case of PCI. Since, the fluctuations in pressure differences in Antarctic coastal region and mid-latitudes (SAM's variability) also modify the pressure distribution that is used to define PCI, so high correlation is expected.

There are differences between the two indices as well. PCI is a semiannual phenomenon whereas SAM has an annual cycle. The SAM influences the strength of the westerlies, while PCI drives katabatic winds in the coastal region, although it also contains zonal variability. Since, SAM and PCI share 38% of observed variance, it further proves our point that $PC1_{500}$ and PCI are both driven by and the variability in Polar Cell is influenced by

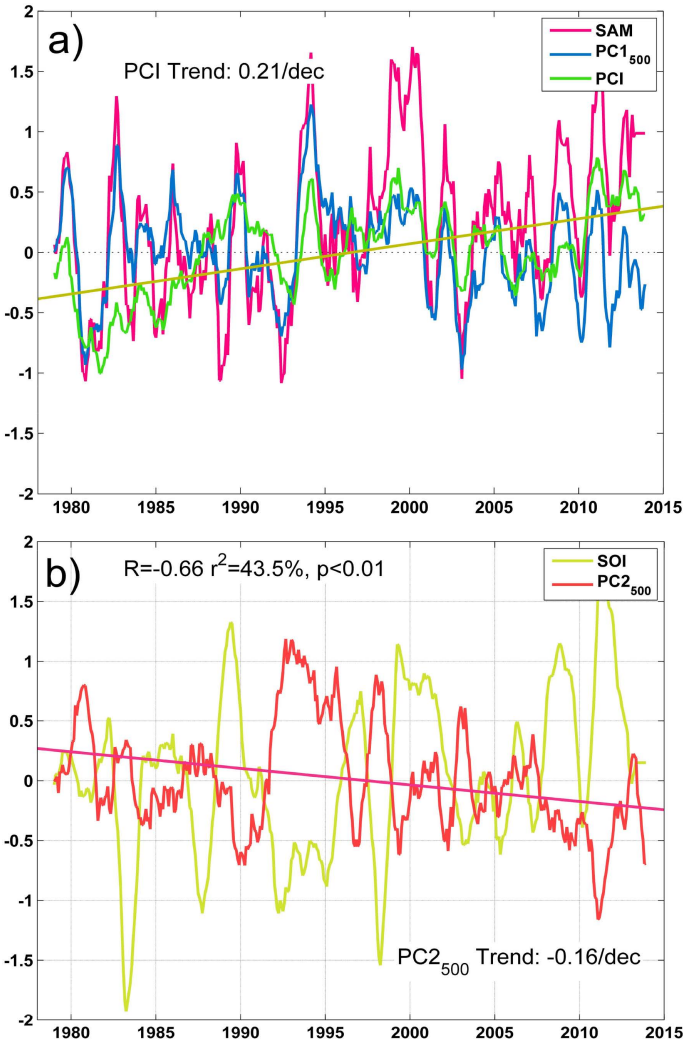

Figure 3. (a) Time-series of SAM, $PC1_{500}$ and PCI, with PCI trend line (in olive green); (b) Time-series of SOI and $PC2_{500}$, with $PC2_{500}$ trend line (in pink).

SAM. Other PCs do not show any significant relationship with SAM.

We also seek to highlight the relationship between variability in Polar Cell and ENSO forcing. The $PC2_{500}$ is negatively correlated ($R = -0.66$, $p < 0.01$) with standardised SOI. Previous studies have also detected positive height anomalies at 500 hPa level over the ABS in response to ENSO events [39] [40]. Overall, $PC2_{500}$ and SOI complement each other closely (**Figure 3(b)**). This is consistent with findings of Mo [6] that second PC (e.g. $PC2_{500}$) is the SH (Polar Cell) is response to warm ENSO events and correlates well with the negative SOI. They pointed out that the ENSO events are primary mechanisms for excitation of second mode of variability in the SH atmosphere

These modes seldom act independently despite the fact that modes are driven by diverse processes and computed from different climate variables. For example, reference [41] found that when an ENSO cold event takes place with the positive SAM, ABSL is intensified. Similarly, the ABS region experiences anomalous high pressure when ENSO warm event is concurrent with the negative phase of the SAM. And these changes in ABSL are shown to affect West Antarctic climate and sea ice around Antarctica [42].

3.5. Impact of Polar Cell Modes on Sea Ice

We evaluate the relevance of each index by the strength of correlation of these indices with the SIC pixels. We

quantify the influences from these climate indices by calculating number significant correlations with indices lag and lead sea ice by 6 months, in order to explore causative impact on each other. Monthly time series were low pass filtered to focus on longer than sub-annual timescales.

Figure 4 shows number of grid points for correlation coefficient significant at $p < 0.01$. The total number of grids was 104,912 (332 × 316) out of which sea ice grids were 82,907. With modes lagging SIC by 1 to 6 months, SAM is less influential than $PC3_{500}$ and PCI, suggesting that the former cannot affect sea ice more than a month in advance (**Figure 4**). $PC1_{500}$ and $PC2_{500}$ modes exhibit more significant correlations than SAM for all lead-lags. SAM is slightly behind $PC1_{500}$ at all times, while the difference between SAM and $PC2_{500}$ is as much as 5 times at 6-month mode lag then narrows at 2-month mode lead but still consistently higher than expectation. Above observations clearly show that SAM is relatively less influential on sea ice than other climate modes. Reference [11] also observed similar results and concluded that local factors have "consistently higher" influence on sea ice than SAM, which confirms that local circulation has major impact on SIC.

Figure 5 shows spatial pattern of peak correlation between these modes and SIC when the former leads the latter by 2 months, except for PCI and $PC3_{500}$ where they lead SIC by 4 and 12 months, respectively. The PCI and $PC1_{500}$ have impact on SIC similar to that of SAM (**Figure S2(b)**), which is expected due to high cross-correlation with SAM. The impact of PCI, $PC1_{500}$ and $PC3_{500}$ on SIC is similar with positive correlation around Antarctic coast, except Weddell Sea. In ABS and Ross Sea, we find significant positive correlation, while negative correlation occurs in Weddell Sea (**Figure 5(a)**, **Figure 5(b)**, **Figure 5(d)**). $PC2_{500}$ strongly projects the Antarctic Dipole (ADP) SIC anomalies in the western Antarctica (**Figure 5(c)**). This correlation pattern results from the observed low similar to ABSL (**Figure 1(b)**), which generates opposite heat fluxes in the Ross Sea and Weddell Sea [27].

As ABS is the region with significant variability in Southern Ocean on the interannual time scale, $PC2_{500}$ represents the largest contribution in ADP regions. The second largest impact comes from the $PC1_{500}$ pattern. As its spatial loading occurs around East Antarctica, Ross Sea and ABS, we point out that its influence on SIC is evenly distributed among the three lobes (**Figure 1(a)**). The correlation pattern from the PCI is quite similar to $PC2_{500}$ in both hemispheres, only the polarity is reversed. The $PC3_{500}$ mode is formed by anomalous low pressure system which creates milder conditions over AP (**Figure 5(d)**). In both hemispheres, $PC1_{500}$ and $PC2_{500}$ patterns generally have higher correlations with SIC than PCI and $PC3_{500}$. Though the influences from all modes

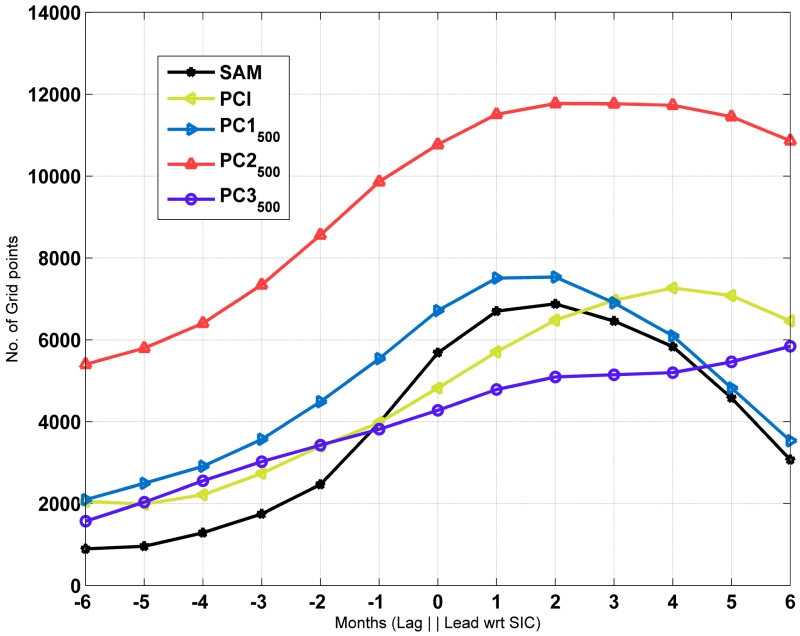

Figure 4. Number of significant correlations of each climate mode ($PC1_{500}$, $PC2_{500}$, $PC3_{500}$, PCI and SAM) with 6 months lag and 6 months lead with respect to SIC (on left-hand side modes are lagging while on right-hand side leading the sea-ice).

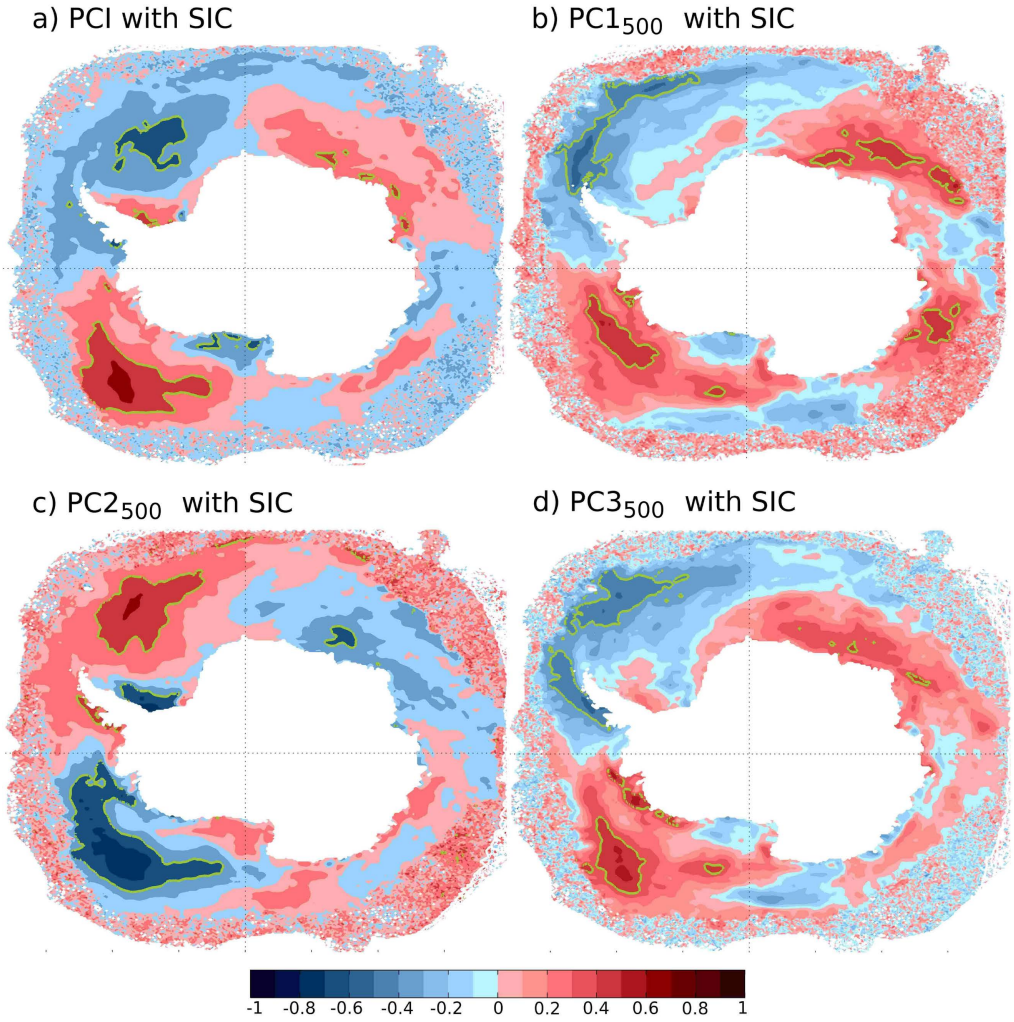

Figure 5. Spatial correlation of (a) PCI, (b) $PC1_{500}$, (c) $PC2_{500}$, and (d) $PC3_{500}$ with a lead of 4, 2, 2 and 12 months, respectively, with sea ice concentration (SIC); regions with values significant at 99% level are enclosed in green contours.

are present in South Western Pacific Ocean, only $PC1_{500}$ has significant impact especially off the coast of Wilkes Land.

The highest number of significant correlations occurs at lead of 2 months for $PC1_{500}$ and $PC2_{500}$ modes, 12 months for $PC3_{500}$, and 4 months for PCI, suggesting that SIC reacts to circulation changes after a pause. This analysis delineates cause and effect relationship between the climate indices and SIC. It is noted that these assessments reflect the influence of the each climate mode on SIC, which may not adequately explain SIC trends observed in individual regions. For example, the largest increase in sea ice is in the Ross Sea with minor contributions from the Weddell Sea and Indian Ocean sector, contrasting with decline in the ABS [43]. These trends cannot be attributed to individual modes as such trends emerge from complex interaction between these modes at different time-scales.

Moreover, our investigation does not point to decadal variability owing to the limited time series. Apart from interannual variability, these climate indices have significant sub-annual variabilities. As aforementioned, $PC2_{500}$ and PCI have the largest signal in autumn and spring, whereas $PC1_{500}$ pattern is dominant in winter (**Figure 2(b)**). To include seasonal variability [44], we repeated the analysis with unfiltered time series. The seasonal correlation patterns were similar to **Figure 5**, but with largely paler magnitude for all modes except for PCI (not shown), suggesting that PCI yields substantial control over sub-annual SIC variability and merit separate study to understand synoptic scale processes.

4. Discussion and Conclusions

In this study, we examined the main characteristics of leading modes of Southern Polar Cell and their relationship with global climate indices along with its impact on Antarctic sea ice. Four climate modes were generated from different atmospheric variables MSLP (PCI) and Z_{500} ($PC1_{500}$, $PC2_{500}$ and $PC3_{500}$). It was observed that the Polar Cell is barotropic and Z_{500} field was used for further investigation as it accounted for more observed variability than other variables. First three dominant modes combined explain nearly 80% of the observed variability. Maximum loading of $PC1_{500}$ occurs at high-plateau regions in the East Antarctica and Marie Byrd Land in the West Antarctica coinciding with high MSLP regions. $PC2_{500}$ pattern is a well documented feature representing ABSL system forming off the coast of West Antarctica and $PC3_{500}$ mode is formed by a low pressure centre over AP.

As expected $PC1_{500}$ is closely related to SAM, which confirms that SAM indeed is dominant atmospheric feature of the SH. Also, PCI is highly correlated with SAM suggesting that latter's signal is present in all atmospheric variables. The $PC2_{500}$ was found to share large amount of variance with ENSO confirming Mo's [6] and related studies. It is observed that PSA pattern of high pressure in the Amundsen Sea, low pressure in the South Atlantic Ocean and east of New Zealand is formed in response to ENSO warm events and vice versa for cold events. They referred PSA pattern as sum of two distinct modes PSA1 and PSA2 which are high- and low-frequency response to the ENSO signal, respectively. However, a recent study by [45] has questioned the existence of PSA1 and PSA2 modes as separate modes due to non-compliance to separation criteria of [46]. If same test is applied to $PC2_{500}$ and $PC3_{500}$, the difference in amount of variance explained by these two is not large enough to satisfy such criterion. However, the existence and uniqueness of a climate mode can be judged by amount of impact it has on other fields. Here, we find that $PC2_{500}$ and $PC3_{500}$ not only separately exist but are driven by different physical processes, testified by unique impact on sea ice.

One of the interesting results is that only two (PCI and $PC2_{500}$) climate indices have significant linear trend over the study period. The observed trend results from simultaneous ABSL deepening and cooling over Antarctica. ABSL deepening is in response to La Nina events [27] [38]. Some studies indicate that Antarctic cooling may have been caused by a combination of positive SAM [47], stratospheric ozone depletion [48] and stratospheric cooling due to CO_2 [49]. Seasons of largest changes [22] in ozone (spring) and wind circulation (summer and autumn) are not synchronised with deepening of the CPT (spring and autumn) suggesting a non-linear relationship. Also PCI and $PC2_{500}$ show clear seasonality of half-yearly cycle strictly following movement of the CPT (**Figure 3**).

Based on the correlation patterns produced by these modes (**Figure 5**), we would anticipate sea ice trends different than current sea ice trends. The correlation maps are very dissimilar to one another and often contradictory as mentioned before. The reported sea ice trends are resultant of complex amalgamation of known and unknown climate modes on different time scales. However, a few points can be noted. All climate modes except $PC2_{500}$ favour sea ice growth in Indian Ocean with strongest impact from $PC1_{500}$. As for the West Pacific Ocean sector only $PC1_{500}$ have significant positive impact, while others modes have mixed influences. Most significant correlations are found in the ADP regions which differentiate one mode from another. All modes except $PC2_{500}$ intensify sea ice dipole in the Weddell Sea and ABS, similar to the response of ENSO cold events (La Nina). However, $PC2_{500}$ response is similar to ENSO warm event (El Nino) as revealed by a strong negative correlation between $PC2_{500}$ and SOI (**Figure 2**).

Current changes in sea ice convey opposite message compared to what can be expected from correlation pattern for SAM (**Figure S2(a)**) or PCI/$PC1_{500}$ modes (**Figure 5(a)**, **Figure 5(b)**). For example, SAM and PCI would favour positive trend in ABS while negative trend in Weddell Sea, on the contrary the current trend is just reverse of that. We argue that large impact from $PC2_{500}$ nullifies the effect of other modes and reverses the polarity of the sea ice trends in the above mentioned regions, resulting in observed sea ice trends [43]. However, the trend is positive for PCI and SAM; and negative for $PC2_{500}$, hence we suggest that current SIC trend in these regions would reverse, provided polarity of trends of these modes remains same. In addition to the spatial patterns of correlation, **Figure 4** reveals that the major air-ice interaction occurs in the forms of proposed climate modes, $PC2_{500}$, $PC1_{500}$, PCI and $PC3_{500}$ in the decreasing order of influence in the interannual time scale.

The interplay of atmosphere and sea ice ensue continuous and delayed response. The continuous response could be due to thermodynamic impact of the surface circulation on the ice, e.g., meridional heat transport, kinetic energy exchanges. For example, PCI could dictate the ocean heat-flux in the open water areas due to its in-

fluence on coastal winds. The lagged reaction would occur through prior conditioning of the ocean (due to e.g. ENSO warm/cold events), which will affect ice growth/decay with finite delay. Reference [27] showed that ENSO signal persists after 3 - 4 seasons in sea ice fields in the ADP regions. Moreover, this work shows that sea ice responds to atmospheric anomalies with a gap, in contrast to marginal ice response to coastal wind forcing at much shorter time scales.

Reference [27] synthesised the evolution and persistence of ADP anomalies in terms of the location and structure of the jets in south-eastern Pacific during ENSO warm and cold events. This study takes this understanding further by suggesting that during El Niño, the subtropical jet is robust and polar front jet weakens in the Pacific basin and vice-versa for La Niña. Therefore, more (less) heat is transported poleward in the South Pacific (South Atlantic) resulting in less (more) sea ice.

The jet stream changes reflect in the strength of Ferrel Cell, which becomes strong in the South Pacific and frail in the South Atlantic during El Niño. On a similar note, we can expect an enhanced Polar Cell in the South Pacific and weakened Polar Cell in the South Atlantic due anomalous heat flux polewards of 70˚S (Fig. 7 in [27]). The changes in polar frontal jet manifest itself as the suppressor of the CPT northward expansion subsequently forming a strong polar vortex [50], which will create stronger pressure gradient across Antarctica (e.g. stronger PCI, $PC2_{500}$) and will have much more impact on sea ice variability.

The new results suggest that ENSO and SAM driven atmospheric modes, especially $PC2_{500}$, have largest impact on Antarctic sea ice changes in the Polar Cell domain. Despite the fact that all these modes are generated distinctly and computed from different atmospheric variables, they mutually interact within the climate system of the SH. The shared impact from these regional climate modes on sea ice and the feedback generated by the tropical ENSO events are not fully comprehended and need additional inquiry. The investigation on PCI should be continued to understand atmospheric impact on seasonal sea ice variability.

Acknowledgements

Sea ice data were obtained from http://nsidc.org/data/nsidc-0051.html and NCEP2 data were downloaded from http://www.esrl.noaa.gov/psd/data/gridded/data.ncep.reanalysis2.html. The NCAR Command Language (NCL, Version 6.2.0) was used to perform EOF analysis and can be found at http://www.ncl.ucar.edu/. This is NCAOR contribution No.: 02/2016.

References

[1] Rogers, J.C. and van Loon, H. (1982) Spatial Variability of Sea-Level Pressure and 500 mb Height Anomalies over the Southern-Hemisphere. *Monthly Weather Review*, **110**, 1375-1392. http://dx.doi.org/10.1175/1520-0493(1982)110<1375:SVOSLP>2.0.CO;2

[2] Gong, D. and Wang, S. (1999) Definition of Antarctic Oscillation Index. *Geophysical Research Letters*, **26**, 459-462. http://dx.doi.org/10.1029/1999GL900003

[3] Kidson, J.W. (1988) Interannual Variations in the Southern Hemisphere Circulation. *Journal of Climate*, **1**, 1177-1198. http://dx.doi.org/10.1175/1520-0442(1988)001<1177:IVITSH>2.0.CO;2

[4] Kidson, J.W. (1988) Indices of the Southern Hemisphere Zonal Wind. *Journal of Climate*, **1**, 183-194. http://dx.doi.org/10.1175/1520-0442(1988)001<0183:IOTSHZ>2.0.CO;2

[5] Karoly, D.J. (1990) The Role of Transient Eddies in Low-Frequency Zonal Variations of the Southern Hemisphere Circulation. *Tellus*, **42A**, 41-50. http://dx.doi.org/10.1034/j.1600-0870.1990.00005.x

[6] Mo, K.C. (2000) Relationships between Low-Frequency Variability in the Southern Hemisphere and Sea Surface Temperature Anomalies. *Journal of Climate*, **13**, 3599-3610. http://dx.doi.org/10.1175/1520-0442(2000)013<3599:RBLFVI>2.0.CO;2

[7] Limpasuvan, V. and Hartmann, D.L. (2000) Wave-Maintained Annular Modes of Climate Variability. *Journal of Climate*, **13**, 4414-4429. http://dx.doi.org/10.1175/1520-0442(2000)013<4414:WMAMOC>2.0.CO;2

[8] Thompson, D.W.J. and Wallace, J.M. (2000) Annular Modes in the Extratropical Circulation, Part I, Month-to-Month Variability. *Journal of Climate*, **13**, 1000-1016. http://dx.doi.org/10.1175/1520-0442(2000)013<1000:AMITEC>2.0.CO;2

[9] Marshall, G.J. (2003) Trends in the Southern Annular Mode from Observations and Reanalyses. *Journal of Climate*, **16**, 4134-4143. http://dx.doi.org/10.1175/1520-0442(2003)016<4134:TITSAM>2.0.CO;2

[10] Liu, J., Curry, J.A. and Martinson, D.G. (2004) Interpretation of recent Antarctic Sea Ice Variability. *Geophysical Re-*

search Letters, **31**, L02205. http://dx.doi.org/10.1029/2003GL018732

[11] Yuan, X. and Li, C. (2008) Climate Modes in Southern High Latitudes and Their Impacts on Antarctic Sea Ice. *Journal of Geophysical Research*, **113**, C06S91. http://dx.doi.org/10.1029/2006jc004067

[12] Holland, P.R. and Kwok, R. (2012) Wind-Driven Trends in Antarctic Sea-Ice Drift. *Nature Geoscience*, **5**, 872-875. http://dx.doi.org/10.1038/ngeo1627

[13] Simpkins, G.R., Ciasto, L.M., Thompson, D.W.J. and England, M.H. (2012) Seasonal Relationships between Large-Scale Climate Variability and Antarctic Sea Ice Concentration. *Journal of Climate*, **25**, 5451-5469. http://dx.doi.org/10.1175/JCLI-D-11-00367.1

[14] Lefebvre, W. and Goosse, H. (2008) An Analysis of the Atmospheric Processes Driving the Largescale Winter Sea Ice Variability in the Southern Ocean. *Journal of Geophysical Research*, **113**, C02004. http://dx.doi.org/10.1029/2006JC004032

[15] Li, X., Holland, D.M., Gerber, E.P. and Yoo, C. (2014) Impacts of the North and Tropical Atlantic Ocean on the Antarctic Peninsula and Sea Ice. *Nature*, **505**, 538-542. http://dx.doi.org/10.1038/nature12945

[16] Renwick, J.A., Kohout, A. and Dean, S. (2012) Atmospheric Forcing of Antarctic Sea Ice on Intraseasonal Time Scales. *Journal of Climate*, **25**, 5962-5975. http://dx.doi.org/10.1038/nature12945

[17] Stammerjohn, S.E., Martinson, D.G., Smith, R.C., Yuan, X. and Rind, D. (2008) Trends in Antarctic Annual Sea Ice Retreat and Advance and Their Relation to El Nino-Southern Oscillation and Southern Annular Mode Variability. *Journal of Geophysical Research*, **113**, C03S90. http://dx.doi.org/10.1029/2007JC004269

[18] Sigmond, M. and Fyfe, J.C. (2010) Has the Ozone Hole Contributed to Increased Antarctic Sea Ice Extent? *Geophysical Research Letters*, **37**, L18502. http://dx.doi.org/10.1029/2010GL044301

[19] van den Broeke, M.R. (1998) The Semi-Annual Oscillation and Antarctic Climate. Part I: Influence on Near Surface Temperature (1957-79). *Antarctic Science*, **10**, 175-183.

[20] van den Broeke, M.R. (2000) The Semi-Annual Oscillation and Antarctic Climate. Part 4: A Note on Sea Ice Cover in the Amundsen and Bellingshausen Seas. *International Journal of Climatology*, **20**, 455-462. http://dx.doi.org/10.1002/(SICI)1097-0088(20000330)20:4<455::AID-JOC482>3.0.CO;2-M

[21] Meehl, G.A. (1991) A Reexamination of the Mechanism of the Semiannual Oscillation in the Southern Hemisphere. *Journal of Climate*, **4**, 911-926. http://dx.doi.org/10.1175/1520-0442(1991)004<0911:AROTMO>2.0.CO;2

[22] Turner, J., Phillips, T., Hosking, J.S., Marshall, G.J. and Orr, A. (2013) The Amundsen Sea Low. *International Journal of Climatology*, **33**, 1818-1829. http://dx.doi.org/10.1002/joc.3558

[23] Steig, E.J., Ding, Q., Battisti, D.S. and Jenkins, A. (2012) Tropical Forcing of Circumpolar Deep Water Inflow and Outlet Glacier Thinning in the Amundsen Sea Embayment, West Antarctica. *Annals of Glaciology*, **53**, 19-28. http://dx.doi.org/10.3189/2012AoG60A110

[24] Cavalieri, D.J., St. Germain, K.M. and Swift, C.T. (1995) Reduction of Weather Effects in the Calculation of Sea-Ice Concentration with the DMSP SSM/I. *Journal of Glaciology*, **41**, 455-464.

[25] Kistler, R., *et al*. (2001) The NCEP-NCAR 50-Year Reanalysis: Monthly Means CD-ROM and Documentation. *Bulletin of the American Meteorological Society*, **82**, 247-267. http://dx.doi.org/10.1175/1520-0477(2001)082<0247:TNNYRM>2.3.CO;2

[26] Fogt, R.L., Jones, J.M. and Renwick, J. (2012) Seasonal Zonal Asymmetries in the Southern Annular Mode and Their Impact on Regional Temperature Anomalies. *Journal of Climate*, **25**, 6253-6270. http://dx.doi.org/10.1175/JCLI-D-11-00474.1

[27] Yuan, X. (2004) ENSO-Related Impacts on Antarctic Sea Ice: Synthesis of Phenomenon and Mechanisms. *Antarctic Science*, **16**, 415-425. http://dx.doi.org/10.1017/S0954102004002238

[28] Lachlan-Cope, T. and Connolley, W. (2006) Teleconnections between the Tropical Pacific and the Amundsen-Bellinghausens Sea: Role of the El Nino/Southern Oscillation. *Journal of Geophysical Research*, **111**, D23101. http://dx.doi.org/10.1029/2005JD006386

[29] Turner, J., Marshall, G. and Lachlan-Cope, T. (1998) Analysis of Synoptic-Scale Low Pressure Systems within the Antarctic Peninsula Sector of the Circumpolar Trough. *International Journal of Climatology*, **18**, 253-280. http://dx.doi.org/10.1002/(SICI)1097-0088(19980315)18:3<253::AID-JOC248>3.0.CO;2-3

[30] van Loon, H. (1967) The Half-Yearly Oscillation in the Middle and High Latitudes and the Coreless Winter. *Journal of the Atmospheric Sciences*, **24**, 472-486. http://dx.doi.org/10.1175/1520-0469(1967)024<0472:THYOIM>2.0.CO;2

[31] van Loon, H. (1984) The Southern Oscillation, Part 3, Associations with the Trades and with the Trough in the Westerlies of the South Pacific Ocean. *Monthly Weather Review*, **112**, 947-954. http://dx.doi.org/10.1175/1520-0493(1984)112<0947:TSOPIA>2.0.CO;2

[32] Walland, D. and Simmonds, I. (1999) Baroclinicity, Meridional Temperature Gradients, and the Southern Semiannual Oscillation. *Journal of Climate*, **12**, 3376-3382. http://dx.doi.org/10.1175/1520-0442(1999)012<3376:BMTGAT>2.0.CO;2

[33] Enomoto, H. and Ohmura, A. (1990) The Influence of Atmospheric Half-Yearly Cycle on the Sea Ice Extent in the Antarctic. *Journal of Geophysical Research*, **95**, 9497-9511. http://dx.doi.org/10.1029/JC095iC06p09497

[34] Arblaster, J.M. and Meehl, G.A. (2006) Contributions of External Forcings to Southern Annular Mode Trends. *Journal of Climate*, **19**, 2896-2905. http://dx.doi.org/10.1175/JCLI3774.1

[35] Turner, J., Colwell, S.R., Marshall, G.J., Lachlan-Cope, T.A., Carelton, A.M., Jones, P.D., Lagun, V., Reid, P.A. and Iagovkina, S. (2005) Antarctic Climate Change during the Last 50 Years. *International Journal of Climatology*, **25**, 279-294. http://dx.doi.org/10.1002/joc.1130

[36] Steig, E.J., Schneider, D.P., Rutherford, S.D., Mann, M.E., Comiso, J.C. and Shindell, D.T. (2009) Warming of the Antarctic Ice-Sheet Surface since the 1957 International Geophysical Year. *Nature*, **457**, 459-462. http://dx.doi.org/10.1038/nature07669

[37] Raphael, M.N., Marshall, G.J., Turner, J., Fogt, R., Schneider, D., Dixon, D.A., Hosking, J.S., Jones, J.M. and Hobbs, W.R. (2015) The Amundsen Sea Low: Variability, Change and Impact on Antarctic Climate. *Bulletin of the American Meteorological Society*, **97**, 111-121. http://dx.doi.org/10.1175/BAMS-D-14-00018.1

[38] Yuan, X. and Martinson, D.G. (2001) The Antarctic Dipole and Its Predictability. *Geophysical Research Letters*, **28**, 3609-3612. http://dx.doi.org/10.1029/2001GL012969

[39] Houseago, R., McGregor, G., King, J.C. and Harangozo, S.A. (1998) Climate Anomaly Wave-Train Patterns Linking Southern Low and High Latitudes during South Pacific Warm and Cold Events. *International Journal of Climatology*, **18**, 1181-1193. http://dx.doi.org/10.1002/(SICI)1097-0088(199809)18:11<1181::AID-JOC332>3.0.CO;2-X

[40] Renwick, J.A. (2005) Persistent Positive Anomalies in the Southern Hemisphere Circulation. *Monthly Weather Review*, **133**, 977-988. http://dx.doi.org/10.1175/MWR2900.1

[41] Fogt, R.L., Bromwich, D.H. and Hines, K.M. (2011) Understanding the SAM Influence on the South Pacific ENSO Teleconnection. *Climate Dynamics*, **36**, 1555-1576. http://dx.doi.org/10.1007/s00382-010-0905-0

[42] Hosking, J.S., Orr, A., Marshall, G.J., Turner, J. and Phillips, T. (2013) The Influence of the Amundsen-Bellingshausen Seas Low on the Climate of West Antarctica and Its Representation in Coupled Climate Model Simulations. *Journal of Climate*, **26**, 6633-6648. http://dx.doi.org/10.1175/JCLI-D-12-00813.1

[43] Parkinson, C.L. and Cavalieri, D.J. (2012) Antarctic Sea Ice Variability and Trends, 1979-2010. *The Cryosphere*, **6**, 871-880. http://dx.doi.org/10.5194/tc-6-871-2012

[44] Holland, P.R. (2014) The Seasonality of Antarctic Sea Ice Trends. *Geophysical Research Letters*, **41**, 4230-4237. http://dx.doi.org/10.1002/2014GL060172

[45] Matthewman, N.J. and Magnusdottir, G. (2012) Clarifying Ambiguity in Intraseasonal Southern Hemisphere Climate Modes during Austral Winter. *Journal of Geophysical Research*, **117**, D03105. http://dx.doi.org/10.1029/2011jd016707

[46] North, G.R., Bell, T.L., Cahalan, R.F. and Moeng, F.J. (1982) Sampling Errors in the Estimation of Empirical Orthogonal Functions. *Monthly Weather Review*, **110**, 699-706. http://dx.doi.org/10.1175/1520-0493(1982)110<0699:SEITEO>2.0.CO;2

[47] Thompson, D.W.J. and Solomon, S. (2002) Interpretation of Recent Southern Hemisphere Climate Changes. *Science*, **296**, 895-899. http://dx.doi.org/10.1126/science.1069270

[48] Gillett, N.P. and Thompson, D.W.J. (2003) Simulation of Recent Southern Hemisphere Climate Change. *Science*, **302**, 273-275. http://dx.doi.org/10.1126/science.1087440

[49] Shindell, D.T. and Schmidt, G.A. (2004) Southern Hemisphere Climate Response to Ozone Changes and Greenhouse Gas Increases. *Geophysical Research Letters*, **31**, L18209. http://dx.doi.org/10.1029/2004gl020724

[50] Hurrell, J.W. and van Loon, H. (1994) A Modulation of the Atmospheric Annual Cycle in the Southern-Hemisphere. *Tellus A*, **46**, 325-338.

Supplementary Figures

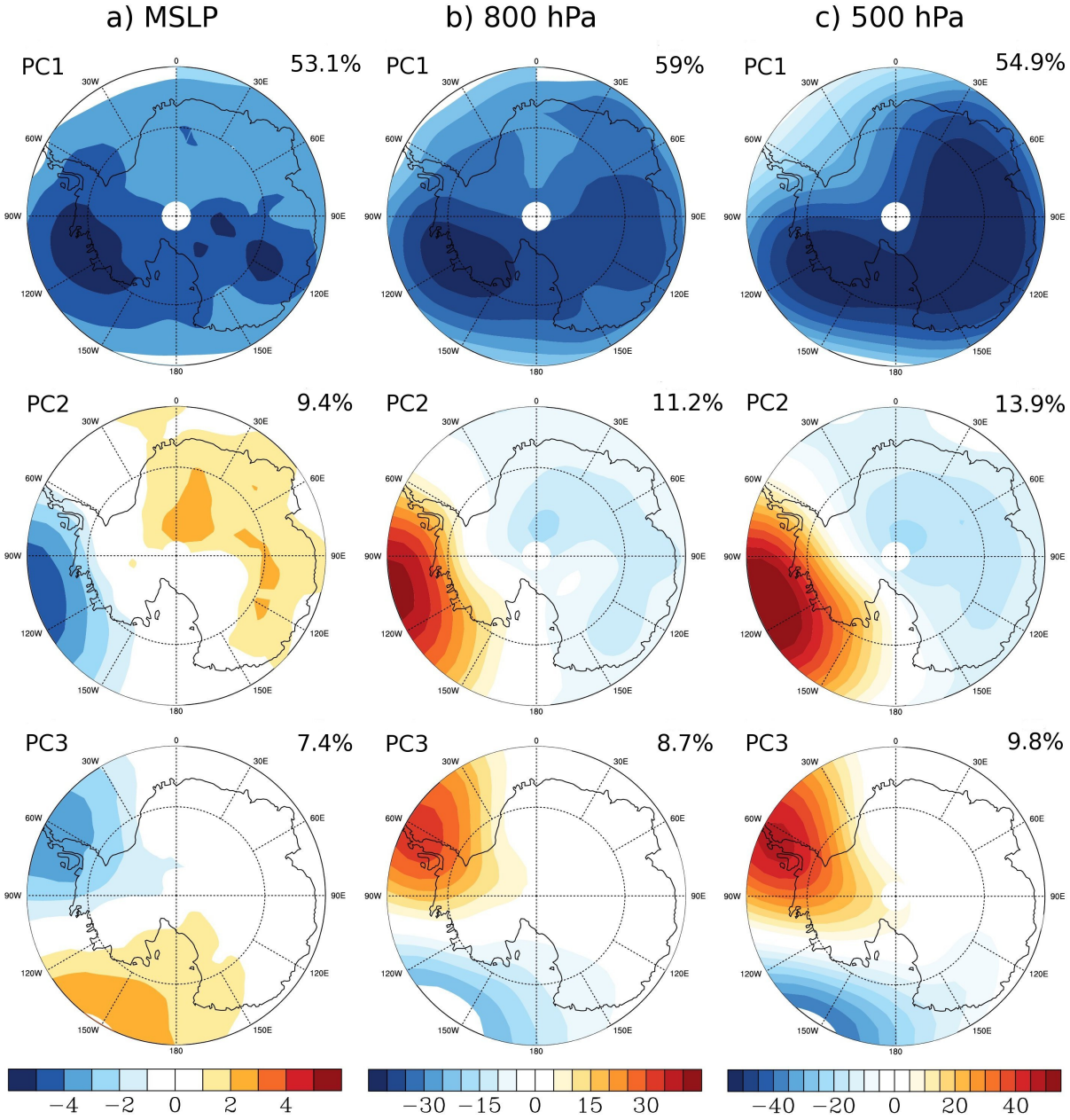

Figure S1. Spatial pattern of first three leading modes of (a) MSLP, (b) Z_{800} (800 hPa level), and (c) Z_{500} (500 hPa level) in the Polar Cell (poleward of 65˚S) with explained variances in percentage.

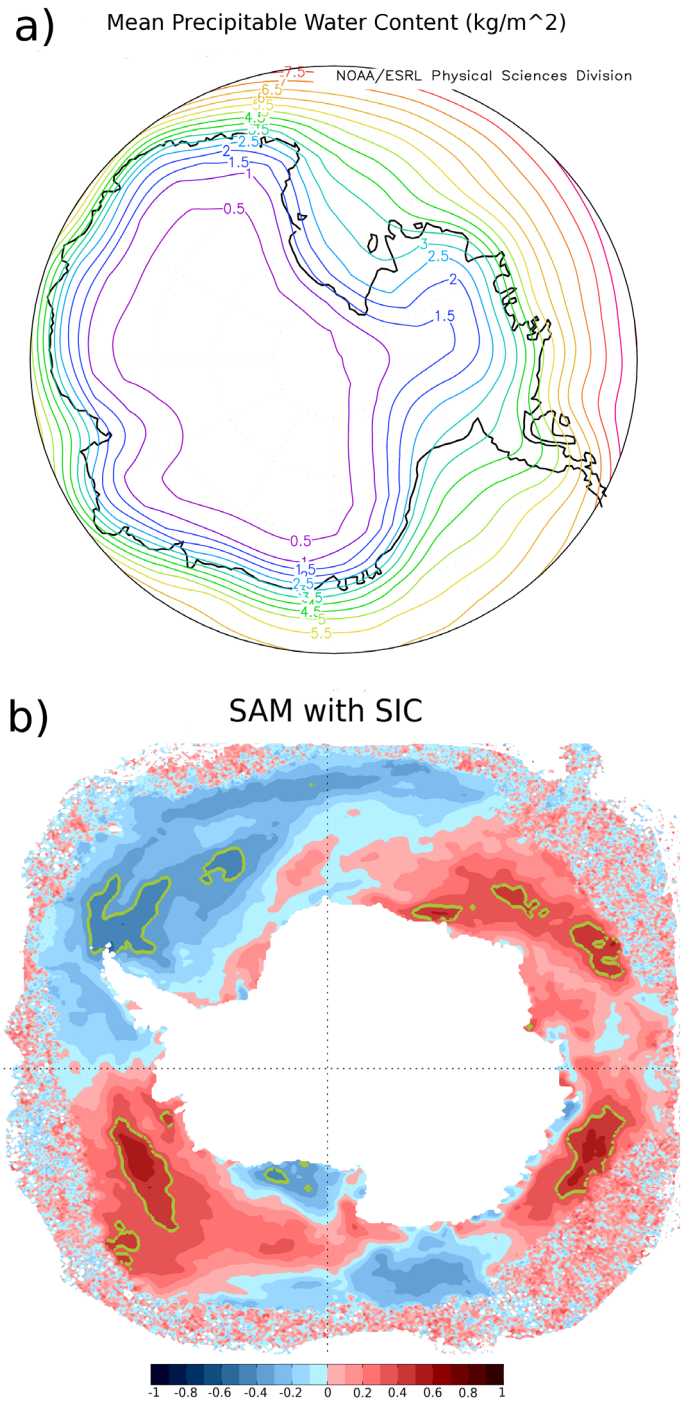

Figure S2. (a) 1979-2013 mean precipitable water content in the air column over Antarctica (source: NOAA); (b) Correlation between SAM with sea ice concentration (SIC); regions where the values are significant at 99% level are enclosed in green contours.